https://doi.org/10.31925/farmacia.2026.2.13 **ORIGINAL ARTICLE**

EFFECTS OF DENOSUMAB COMBINED WITH CALCITRIOL ON BONE METABOLISM AND REFRACTURE RATE IN ELDERLY PATIENTS WITH OSTEOPOROTIC VERTEBRAL COMPRESSION FRACTURES AFTER PERCUTANEOUS KYPHOPLASTY

SAI YU, ZEBING ZHANG, TAISHAN ZHU, ZEYU YE, LEMING LIAO *

[1]*Department of Orthopedics, Fuyang Campus of Zhejiang Provincial People's Hospital (The First People's Hospital of Fuyang), Hangzhou, 311400, Zhejiang, China*

**corresponding author: rickshakespeare@126.com*

Manuscript received: January 2026

Abstract

This retrospective study evaluated the effects of denosumab combined with calcitriol on bone metabolism, vertebral recovery, and refracture risk in elderly patients with osteoporotic vertebral compression fractures (OVCF) after percutaneous kyphoplasty (PKP). A total of 152 patients were divided into a control group (calcitriol, n = 76) and an observation group (denosumab plus calcitriol, n = 76) for 12 months. Radiological parameters and bone metabolism markers were assessed preoperatively and up to 12 months postoperatively. The observation group showed significantly improved vertebral anterior height recovery (82.3 ± 6.1% *vs*. 73.5 ± 7.8%), better Cobb angle correction, and a lower cement leakage rate (7.89% *vs*. 14.47%). At 6 and 12 months, bone mineral density and formation markers (BGP, PINP) were higher, while β-CTX levels were lower ($p < 0.05$). The refracture rate was significantly reduced (5.26% *vs*. 17.11%) without differences in adverse reactions. Vertebral recovery correlated positively with bone formation markers and negatively with resorption markers. Denosumab combined with calcitriol improves bone metabolism, enhances vertebral restoration, and reduces refracture risk, demonstrating favorable efficacy and safety in elderly OVCF patients after PKP.

Rezumat

Acest studiu retrospectiv a evaluat efectele asocierii dintre denosumab și calcitriol asupra metabolismului osos, recuperării morfologiei vertebrale și riscului de refractură la pacienții vârstnici cu fracturi vertebrale osteoporotice prin compresie (OVCF) după cifoplastie percutană (PKP). Un total de 152 de pacienți au fost împărțiți într-un lot martor (calcitriol, n = 76) și un lot de studiu (denosumab plus calcitriol, n = 76), urmăriți timp de 12 luni. Parametrii imagistici și markerii metabolismului osos au fost evaluați preoperator și postoperator până la 12 luni. Lotul de studiu a prezentat o recuperare semnificativ mai bună a înălțimii anterioare vertebrale (82,3 ± 6,1% *vs*. 73,5 ± 7,8%), o corecție superioară a unghiului Cobb și o rată mai redusă a extravazării cimentului (7,89% *vs*. 14,47%). La 6 și 12 luni, densitatea minerală osoasă și markerii formării osoase (BGP, PINP) au fost mai crescute, iar valorile β-CTX au fost mai scăzute ($p < 0,05$). Rata refracturilor a fost semnificativ redusă (5,26% *vs*. 17,11%), fără diferențe privind reacțiile adverse. Asocierea denosumab - calcitriol a îmbunătățit metabolismul osos, a favorizat restaurarea vertebrală și a redus riscul de refractură.

Keywords: denosumab, calcitriol, OVCF, PKP, MRI

Introduction

Osteoporosis is a common systemic skeletal disease in the elderly population, and osteoporotic vertebral compression fractures (OVCF) often cause severe pain, spinal deformity, and restricted movement (1, 2). Percutaneous kyphoplasty (PKP) can rapidly stabilize the vertebrae and relieve pain by injecting bone cement, but the residual bone metabolism imbalance and vertebral biomechanical changes after surgery can still lead to refracture of adjacent vertebrae (3, 4). Therefore, postoperative drug intervention to improve bone metabolism and reduce refracture risk has become a key direction in clinical research.

In recent years, the combined use of anti-resorptive drugs and bone-forming drugs has gradually attracted attention. Denosumab is a humanized monoclonal antibody that specifically binds to receptor activator of nuclear factor-κB ligand (RANKL) and blocks its interaction with the RANK receptor on the surface of osteoclasts, thereby inhibiting the differentiation, activation, and survival of osteoclasts, effectively reducing bone resorption and increasing bone density (5). This drug is mainly used to treat postmenopausal osteoporosis (6), bone metastasis of malignant tumors (7) and giant cell tumors of bone (8), with a clinical manifestation of significantly reducing fracture risk. Calcitriol is the active metabolite of vitamin D3 after hydroxylation in the liver and kidneys, which can directly bind to the vitamin D

receptor in the nucleus of target cells and regulate gene expression. It promotes the synthesis of calcium-binding proteins in intestinal epithelial cells, enhances calcium and phosphorus absorption, stimulates osteoblast differentiation and bone matrix mineralization, and indirectly inhibits parathyroid hormone (PTH) secretion due to increased blood calcium levels, forming a negative feedback regulation (9). It is clinically used for the treatment of secondary hyperparathyroidism in chronic kidney disease (10), hypoparathyroidism (11) and osteoporosis (12). Compared with ordinary vitamin D, it does not require metabolic activation and has a stronger effect, but strict monitoring of blood calcium, phosphorus, and renal function is needed to avoid risks such as hypercalcemia and ectopic calcification (13). Studies have shown that monotherapy with calcitriol can effectively improve hypocalcemia and abnormal bone turnover caused by chronic kidney disease or parathyroid dysfunction (14).

Existing studies have mostly focused on the improvement of short-term bone metabolism markers, lacking dynamic radiological assessment of postoperative vertebral shape recovery and bone healing quality, especially long-term tracking based on MRI (15, 16). Traditional radiological methods such as X-ray can assess vertebral height and cement distribution, but they are not sensitive to early bone marrow edema, trabecular microstructural changes, and bone healing process. CT has higher resolution, but the risk of radiation exposure limits its repeated application (17). In contrast, MRI, with its advantages of no radiation, multi-parameter imaging, and high soft tissue resolution, can clearly display the extent of bone marrow edema after vertebral fracture, the integrity of the endplates, and the fusion state of the cement-bone interface, providing an important basis for assessing postoperative bone healing quality and predicting refracture risk (18). In addition, the detection rate of cement leakage by MRI is significantly higher than that by X-ray, especially for early diagnosis of leakage in paravertebral soft tissues or within the spinal canal, which helps guide timely clinical intervention (19).

This study focused on elderly patients with OVCF, who were treated with denosumab and calcitriol in combination after PKP. Through a 12-month follow-up, combined with MRI radiological parameters (vertebral anterior height recovery rate, Cobb angle, cement leakage) and biochemical markers of bone metabolism (BMD, BGP, PINP, β-CTX), the study systematically explored the comprehensive effects of combined therapy on postoperative bone metabolism reconstruction, vertebral shape recovery, and refracture rate, in order to provide multidimensional evidence-based support for optimizing postoperative management in elderly patients with OVCF.

Materials and Methods

Clinical data

This retrospective study analyzed 152 elderly patients with OVCF who underwent PKP at Zhejiang Provincial People's Hospital, Zhejiang, China between January 2020 and January 2024. Patients were identified through electronic medical records and were divided into a control group (n = 76) and an observation group (n = 76) based on the actual postoperative medication regimen they received.

In observation group, there were 42 males and 34 females with an age range of 60 - 88 years (mean age 64.32 ± 4.12 years), and a time from fracture to admission of 2.1 - 5.4 hours (mean 3.17 ± 1.31 hours). In control group, there were 36 males and 40 females with an age range of 61 - 87 years (mean age 65.27 ± 4.23 years), and a time from fracture to admission of 2.5 - 5.8 hours (mean 3.64 ± 1.46 hours). There were no visible distinctions in clinical data between the two groups ($p > 0.05$). The study was approved by Ethics Committee of Zhejiang Provincial People's Hospital (Zhejiang, China). All participants agreed to sign informed consent forms with the consent of their family members.

Inclusion criteria: 1. Compliance with the *Chinese Expert Consensus on Secondary Prevention of Osteoporotic Fractures* (20), individuals confirmed by clinical and laboratory examinations; 2. Age ≥ 60 years, individuals meeting the WHO diagnostic criteria for osteoporosis (21) (BMD T-score ≤ -2.5); 3. Single-level fresh thoracolumbar OVCF (fracture time < 3 weeks), individuals confirmed by MRI with bone marrow edema; 4. Successful PKP surgery with bone cement injection volume of 2.5 - 4.0 mL; 5. No history of severe cardiovascular, hepatic, or renal insufficiency or malignancy.

Exclusion criteria: 1. Pathological fractures (*e.g.,* due to tumors or infections); 2. Presence of autoimmune diseases; 3. Severe dysfunction of vital organs such as heart, liver, or kidneys; 4. History of previous vertebral surgery or spinal deformity; (5) Allergy to denosumab or calcitriol; 6. Use of bisphosphonates, hormones affecting bone metabolism within the past 3 months; 7. Presence of psychiatric disorders or inability to cooperate with treatment; 8. Lost to follow-up and self-discontinued treatment.

Treatment protocol

Control group: Calcitriol soft capsules (0.25 μg/1 capsule; Catalent Germany Eberbach GmbH, Germany) were administered orally starting on the third day after surgery, in doses of 0.25 μg *per* administration, two times/day, for a continuous treatment period of 12 months, 600 mg of calcium carbonate was supplemented daily (600 mg/tablet; Wyeth Pharmaceutical Co., Ltd., China).

Observation group: On the basis of control group, denosumab (XGEVA, Amgen Manufacturing

Limited, USA) was administered via subcutaneous injection one week after surgery. Each injection was 60 mg, once every 6 months, a total of two injections, for a continuous treatment period of 12 months.

All subjects received standardized rehabilitation training after surgery, including axial turning, lumbodorsal muscles exercises, and progressive weight-bearing guidance.

Radiological assessment

Dynamic monitoring was performed using a SIGNA Architect AIR 3.0T MRI (GE Medical Systems, Milwaukee, WI, USA): repetition time (TR) = 500 ms, echo time (TE) = 10 ms, slice thickness = 3 mm, matrix = 320×256; T2WI: TR = 3000 ms, TE = 100 ms, slice thickness = 3 mm, matrix = 320×256; Short-tau inversion recovery (STIR) sequence: TR = 4000 ms, TE = 60 ms, inversion time (TI) = 160 ms, slice thickness = 3 mm, matrix = 256×192. All sequences were centered on the fractured vertebra, and sagittal and axial images were obtained, with the scanning range covering two adjacent normal vertebrae above and below. The assessment time points were pre-operation, immediately post-operation, 6 months, and 12 months.

Vertebral anterior height recovery rate was assessed. On the mid-sagittal T2WI images, the anterior height of the fractured vertebra (Hf) and the anterior height of the adjacent normal vertebra (Hn) (selected from the upper or lower non-fractured vertebra) were measured separately. The calculation equation is as follows:

$$Recovery\ rate(\%) = \frac{H_f}{H_n} \times 100\%$$

If degeneration or old fractures were present in adjacent vertebrae, the nearest vertebra without abnormalities to the fractured vertebra was selected as the reference.

To measure Cobb angle, on the sagittal T2WI images, tangents were drawn along the upper and lower endplates of the fractured vertebra, and the angle between the two tangents was measured. The built-in angle measurement tool of the Siemens Syngo Via workstation (version VB60, Siemens Healthineers, Erlangen, Germany) was used, with precision to 0.1.

To determine cement leakage, according to the grading system recommended by the International Society for the Advancement of Spine Surgery, combined with multiplanar reconstruction on MRI to assess the extent of leakage: Grade 0: No leakage, with cement completely confined within the vertebral body; Grade 1: Paravertebral or intervertebral leakage, with the largest diameter < 2 mm; Grade 2: Leakage ≥ 2 mm, or involvement of the spinal canal or neural foramen. The location of leakage (paravertebral, intervertebral, or intraspinal) was determined by combining axial and sagittal images.

All imaging data were independently analyzed by two radiologists with over ten years of experience in spinal imaging diagnosis, using a double-blind method (the evaluators were unaware of patient grouping and treatment information). In cases of disagreement on the imaging results, a third expert was consulted for arbitration.

Detection of bone metabolism indicators

Fasting venous blood was collected preoperatively, at six months postoperatively, and at twelve months postoperatively to detect the following indicators.

Bone mineral density (BMD) was measured. Dual-energy X-ray absorptiometry (DXA; Hologic Discovery Wi, software version Apex 5.6.0.5, Hologic Inc., Marlborough, MA, USA) was used. The lumbar spine (L1-L4) and the left femoral neck were scanned. Subjects were placed in the supine position with the midline of the spine aligned with the long axis of the scanning bed, and the hip joint was internally rotated by 15° to standardize the positioning of the femoral neck. The lumbar spine was scanned for five minutes, and the femoral neck for three minutes. The same certified technician operated the device, and the software automatically calculated the BMD value (g/cm²) to three decimal places. The device was calibrated daily using a standard phantom (Hologic Anthropomorphic Spine Phantom, Hologic Inc., USA) before scanning, with a coefficient of variation (CV) of less than 1.0%.

To detect serum BGP, electrochemiluminescence immunoassay (ECLIA) was used, with a Roche Cobas e601 fully automatic immunoassay analyzer (Roche Diagnostics, Basel, Switzerland) and the corresponding reagent kit (Roche Diagnostics) to detect BGP.

ELISA was used to detect propeptide of type I procollagen (PINP), bone alkaline phosphatase (BALP), β-CrossLaps (β-CTX). The ELISA kits (including Human PINP ELISA Kit (SEA467Hu), human BALP ELISA Kit (SEA065Hu), and human β-CTX ELISA Kit (CEA665Hu) were purchased from Cloud-Clone Corp (Katy, TX, USA), and the tests were conducted strictly according to the instructions.

Analysis of outcome indicators

Clinical efficacy assessment was conducted. A comprehensive evaluation was conducted at the 12-month postoperative follow-up, integrating patient symptoms, imaging findings, and laboratory indicators. The outcomes were graded as excellent, effective, or ineffective, with the criteria established based on principles referenced from previous clinical studies on osteoporosis.

Excellent: all of the following criteria must be met: 1. Symptoms: postoperative pain is essentially resolved (VAS score ≤ 2). 2. Function: quality of life is significantly restored (SF-36 score improved by ≥80% from baseline, or its physical component summary score > 70). 3. Imaging: good bone healing at the fracture site (MRI shows continuous trabeculae bridging the fracture line); vertebral anterior height

restoration rate ≥ 70%; and local kyphotic Cobb angle change < 3° compared to immediately postoperatively, indicating no significant loss of correction. 4. Bone Metabolism: bone formation marker levels (BGP and/or PINP) increased by ≥50% from baseline, and bone resorption marker levels (β-CTX) decreased by ≥30% from baseline.

Effective: at least three of the following criteria must be met, including at least one "symptom/function" criterion: 1. Symptom/Function: significant reduction in postoperative pain (VAS score decreased by ≥ 4 points from baseline); or moderate improvement in quality of life (SF-36 score improved by 50% - 79% from baseline). 2. Imaging: vertebral anterior height restoration rate ≥ 50%; fracture line appears blurred. 3. Bone metabolism: bone formation marker levels (BGP and/or PINP) increased by 25% - 49% from baseline, and/or bone resorption marker levels (β-CTX) decreased by 15% - 29% from baseline.

Ineffective: any of the following conditions apply: Failure to meet the above "Effective" criteria; occurrence of new vertebral or non-vertebral fragility fractures; occurrence of severe complications related to the surgery or medication; worsening pain or functional status.

The overall effective rate was calculated as: (Number of Excellent cases + Number of Effective cases) / Total number of cases × 100%.

The dynamic changes in bone metabolism indicators (BMD, BGP, PINP, β-CTX, BALP) at immediate postoperation, 6 months, and 12 months were analyzed.

The lumbar spine BMD and femoral neck BMD at immediate postoperation, six months, and twelve months were analyzed.

Radiological parameters (vertebral anterior height recovery rate, Cobb angle correction degree, cement leakage rate) were compared.

The refracture rate (new vertebral or non-vertebral fractures) and adverse reactions (hypocalcemia, gastrointestinal reactions, etc.) at twelve months were recorded.

Statistical analysis

Statistical analysis was performed using SPSS 26.0 (IBM Corporation, Armonk, NY, USA). The normality of continuous variables was assessed using the Shapiro-Wilk test. Data conforming to a normal distribution are presented as mean ± standard deviation and were compared between groups using the independent samples t-test. Data not conforming to a normal distribution were presented as median (interquartile range) and were compared using the Mann-Whitney U test. Categorical data were expressed as number (percentage) and were compared using the χ^2 test or Fisher's exact test (when the theoretical frequency was < 5). Correlations between imaging parameters and bone metabolic markers were analyzed using Pearson correlation analysis. All statistical tests were two-sided, and a p-value < 0.05 was considered statistically significant.

Results and Discussion

Contrast of clinical efficacy

In observation group (n = 76), marked improvement was observed in 40 cases (54.05%), improvement in 28 cases (37.84%), and in improvement in 6 cases (8.11%). The total number of effective cases was 68, yielding an overall effective rate of 91.89%.

In control group (n = 76), marked improvement was observed in 22 cases (30.14%), moderate improvement in 30 cases (41.10%), and no improvement in 21 cases (28.77%), with a total of 52 effective cases and a total effective rate of 71.23%. The total effective rate in observation group was significantly higher as against control group (91.89% *vs*. 71.23%, $\chi^2 = 12.631$, p = 0.001) (Figure 1).

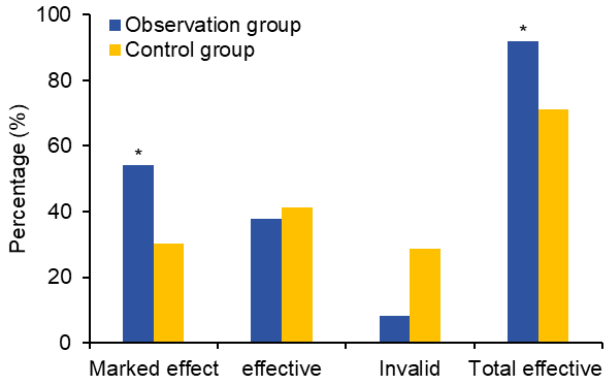

Figure 1.
Contrast of clinical efficacy. *As against control group, p < 0.05

Contrast of bone metabolism-related indicators

In Figure 2A, the preoperative BGP in observation group was (19.2 ± 4.5) ng/mL, at 6 months postoperatively it was (36.6 ± 6.2) ng/mL, and at 12 months postoperatively it was (44.3 ± 6.7) ng/mL. In control group, the preoperative BGP was (18.9 ± 3.8)

ng/mL, at 6 months postoperatively it was (29.4 ± 5.8) ng/mL, and at 12 months postoperatively it was (32.9 ± 7.2) ng/mL. No visible distinction was noted in preoperative BGP in the subjects ($p > 0.05$). At 6 and 12 months postoperatively, BGP was significantly higher than preoperatively, and at 12 months postoperatively it was significantly higher than at 6 months postoperatively; The BGP in observation group at 12 months postoperatively was significantly higher as against control group ($p < 0.05$).

In Figure 2B, the preoperative PINP in observation group was (23.6 ± 4.7) ng/mL, at 6 months postoperatively it was (49.3 ± 9.1) ng/mL, and at 12 months postoperatively it was (56.7 ± 11.4) ng/mL. In control group, the preoperative PINP was (22.9 ± 4.6) ng/mL, at 6 months postoperatively it was (38.9 ± 8.7) ng/mL, and at 12 months postoperatively it was (41.5 ± 8.8) ng/mL. No visible distinction was noted in preoperative PINP in the subjects ($p > 0.05$). At 6 and 12 months postoperatively, PINP was significantly higher than preoperatively, and at 12 months postoperatively it was significantly higher than at 6 months postoperatively. The PINP in observation group at 12 months postoperatively was significantly higher as against control group ($p < 0.05$).

In Figure 2C, the preoperative β-CTX in observation group was (0.69 ± 0.19) ng/mL, at 6 months postoperatively it was (0.36 ± 0.18) ng/mL, and at 12 months postoperatively it was (0.26 ± 0.12) ng/mL. In control group, the preoperative β-CTX was (0.66 ± 0.18) ng/mL, at 6 months postoperatively it was (0.57 ± 0.15) ng/mL, and at 12 months postoperatively it was (0.43 ± 0.16) ng/mL. The β-CTX in the subjects showed a downward trend. No visible distinction was noted in preoperative β-CTX in the subjects ($p > 0.05$). At 6 and 12 months postoperatively, β-CTX was significantly lower than preoperatively, and at 12 months postoperatively it was significantly higher than at 6 months postoperatively. The β-CTX in observation group at 12 months postoperatively was significantly lower as against control group ($p < 0.05$).

In Figure 2D, the preoperative BALP in observation group was (25.2 ± 4.8) U/L, at 6 months postoperatively it was (38.5 ± 6.7) U/L, and at 12 months postoperatively it was (45.1 ± 7.9) U/L. In control group, the preoperative BALP was (24.9 ± 5.1) U/L, at 6 months postoperatively it was (30.2 ± 5.9) U/L, and at 12 months postoperatively it was (33.6 ± 6.4) U/L. No visible distinction was noted in preoperative BALP in the subjects ($p > 0.05$). At 6 and 12 months postoperatively, BALP was markedly higher than preoperatively, and at 12 months postoperatively it was markedly higher than at 6 months postoperatively. The BALP in observation group at 12 months postoperatively was markedly higher as against control group ($p < 0.05$).

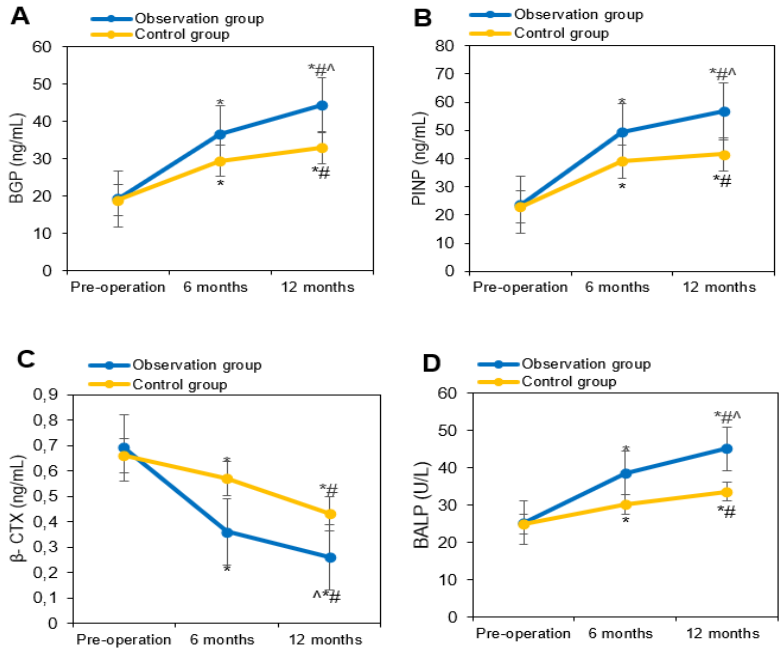

Figure 2.

Contrast of bone metabolism-related indicators. (A) BGP; (B) PINP; (C) β-CTX; (D) BALP. *As against pre-operation in the same group, $p < 0.05$; #as against 6 months, $p < 0.05$; ^as against control group, $p < 0.05$

Contrast of lumbar spine and femoral neck BMD

In Figure 3A, the preoperative lumbar spine BMD growth rate in observation group was (-3.1 ± 0.5)%, at 6 months postoperatively it was (8.2 ± 1.5)%, and at 12 months postoperatively it was (13.5 ± 2.1)%. In control group, the preoperative lumbar spine

BMD was (-3.0 ± 0.6)%, at 6 months postoperatively it was (4.3 ± 1.2)%, and at 12 months postoperatively it was (6.7 ± 1.8)%. In Figure 3B, the preoperative femoral neck BMD in observation group was (-2.8 ± 0.3)%, at 6 months postoperatively it was (6.7 ± 1.4)%, and at 12 months postoperatively it was (9.9 ± 1.7)%. In control group, the preoperative femoral neck BMD was (-2.9 ± 0.5)%, at 6 months postoperatively it was (3.1 ± 1.0)%, and at 12 months postoperatively it was (5.2 ± 1.4)%. No visible distinctions were noted in preoperative lumbar spine BMD growth rate and femoral neck BMD growth rate in the subjects ($p > 0.05$). At 6 and 12 months postoperatively, BMD was markedly higher than preoperatively, and at 12 months postoperatively it was markedly higher than at 6 months postoperatively; The lumbar spine BMD growth rate and femoral neck BMD growth rate in observation group at 12 months postoperatively were markedly higher than those in control group ($p < 0.05$).

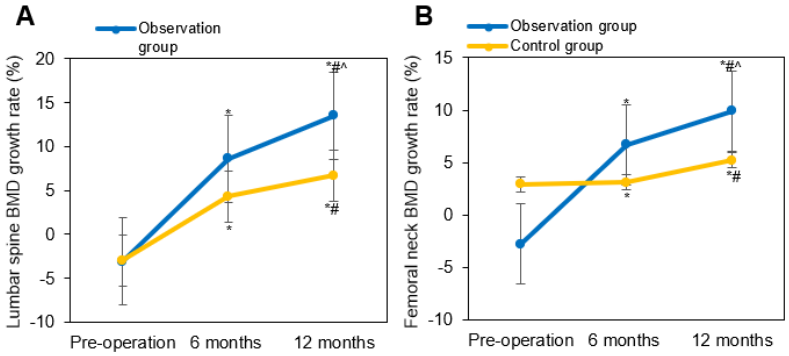

Figure 3.

Comparison results of lumbar spine BMD growth rate and femoral neck BMD growth rate. (A) lumbar spine BMD growth rate; (B) Femoral neck bone growth rate. *As against pre-operation, $p < 0.05$; #as against 6 months, $p < 0.05$; ^as against control group, $p < 0.05$

MRI radiological assessment

The dynamic changes in the Cobb angle for both groups are detailed in Table II. In Figure 4A, the Cobb angle was significantly corrected immediately postoperatively in both groups compared to preoperative values (all $p < 0.05$). Throughout the follow-up period, the Cobb angle in the observation group remained stable at both 6 and 12 months. In contrast, the Cobb angle in the control group gradually increased, indicating a loss of correction over time. The Cobb angle in the control group was significantly larger than that in the observation group at both 6 months (15.9 ± 3.8° *vs*. 12.7 ± 3.0°, $p < 0.05$) and 12 months postoperatively (18.7 ± 4.3° *vs*. 12.8 ± 3.1°, $p < 0.05$).

In Figure 4B, cement leakage, the leakage rate in observation group was 7.89% (6/76), markedly lower as against control group at 14.47% (11/76) ($p = 0.042$), and all leakages in observation group were grade 1, while control group had 5 cases of grade 2 leakage. In Figure 4C, there was no visible distinction in the vertebral anterior height recovery rate in the subjects immediately postoperatively ($p > 0.05$); at 6 and 12 months postoperatively, the recovery rates in observation group were (82.3 ± 6.1)% and (80.5 ± 5.8)%, respectively, markedly higher than those in control group at (73.5 ± 7.8)% and (68.2 ± 6.9)% ($p < 0.05$).

Figure 5 (A-D) show the sagittal MRI images of the lumbar spine from an 86-year-old female patient in the control group before and after percutaneous vertebroplasty at different time points. Figure 5A (preoperative) clearly displays the baseline pathological conditions, including vertebral fracture morphology, osteoporotic changes, and significant bone marrow edema signals. Figure 5B (immediately postoperative) shows the assessment of the immediate surgical outcome, showing partial recovery of vertebral height, distribution of bone cement within the vertebral body, and no obvious signs of cement leakage. Figure 5C (6 months postoperative) shows the assessment of mid-term recovery, with images showing improved bone metabolic activity, stable positioning of the bone cement, no significant displacement, and the ongoing process of fracture healing. Figure 5D (12 months postoperative) shows the assessment of long-term efficacy, with imaging confirming continued bone structural recovery, good integration of bone cement with host bone, suggesting the stability of the therapeutic effect.

Figure 5 (E-H) show the sagittal MRI images of the lumbar spine from a 65-year-old female patient in the experimental group at the same time points. Figure 5E (preoperative) displays baseline pathological features similar to the control group, including vertebral fracture, osteoporosis, and bone marrow edema. Figure 5F (immediately postoperative) shows

satisfactory vertebral reduction, good distribution of bone cement, and no signs of leakage. Figure 5G (6 months postoperative) shows more significant improvement in bone metabolism, excellent stability of the bone cement, and clear signs of bone healing. Figure 5H (12 months postoperative) indicates further recovery of bone structure, more ideal integration of bone cement, and stable long-term efficacy.

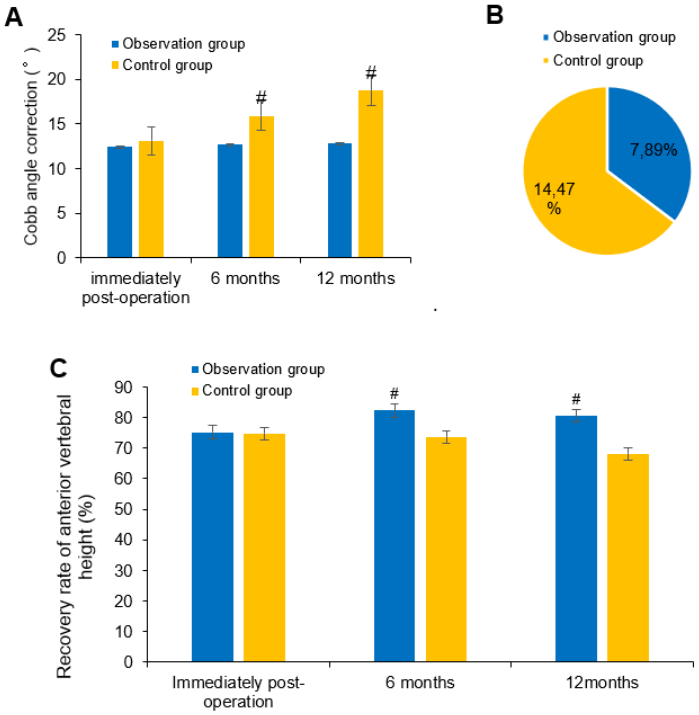

Figure 4.

Contrast of imaging-related indicators in subjects. (A) contrast of Cobb angle correction; (B) contrast of cement leakage; (C) contrast of vertebral anterior height recovery rate. #As against control group, $p < 0.05$; *as against immediately post-operation, $p < 0.05$

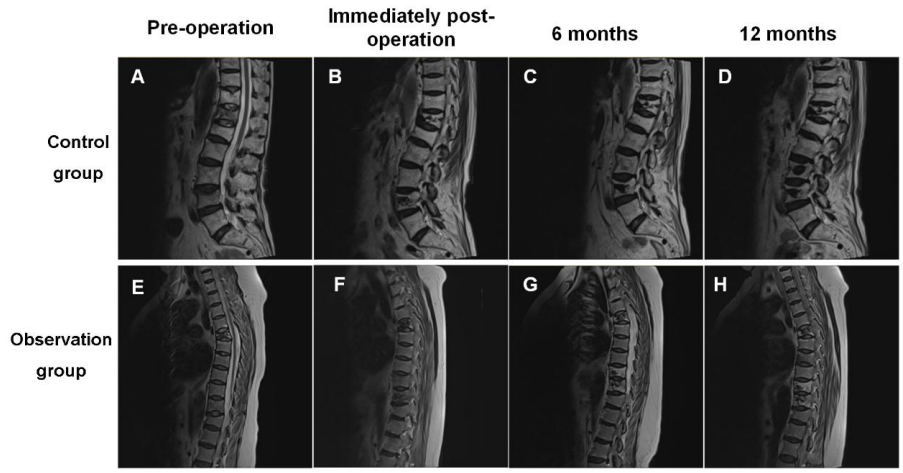

Figure 5.

MRI imaging follow-up assessment. A: preoperative of the control group; B: immediate postoperative of the control group; C: 6 months postoperative of the control group; D: 12 months postoperative of the control group; E: preoperative of the observation group; F: immediate postoperative of the observation group; G: 6 months postoperative of the observation group; H: 12 months postoperative of the observation group

Correlation analysis between MRI radiological parameters and bone metabolism indicators

At 12 months postoperatively, the correlation between radiological parameters and bone metabolism indicators was analyzed (Table I). The vertebral height recovery rate was positively correlated with bone formation markers (BGP, PINP, BALP, BMD) and had negative correlation with β-CTX. The

degree of Cobb angle degeneration (increase in angle) was negatively correlated with bone formation markers, and positively correlated with bone the resorption marker. The vertebral anterior height recovery rate was markedly positively correlated with BALP ($r = 0.463$, $p < 0.001$), indicating that enhanced osteogenic activity promotes vertebral shape recovery. The change in Cobb angle was markedly negatively correlated with BALP ($r = -0.375$, $p = 0.005$), suggesting that high osteogenic activity can slow the progression of kyphosis.

Table I

Correlation analysis between radiological parameters and bone metabolism indicators (at 12 months postoperatively)

Radiological parameters	BGP	PINP	β-CTX	BALP	Lumbar spine BMD	Femoral neck BMD
Vertebral anterior height recovery rate						
r	0.523	0.486	-0.417	0.463	0.383	0.461
p value	0.001	0.001	0.002	0.001	0.004	0.011
Cobb angle change						
r	-0.398	-0.362	0.304	-0.375	-0.395	-0.353
p value	0.003	0.007	0.018	0.004	0.003	**0.015**

Note: BGP, bone gla protein; PINP, procollagen type I N-terminal propeptide; β-CTX, β-C-terminal telopeptide of type I collagen; BALP, bone-specific alkaline phosphatase; BMD, bone mineral density. All p values are derived from Pearson correlation analysis.

Re-fracture rate

At 12 months postoperatively, in observation group, 3 new vertebral fractures (3.95%) and 1 non-vertebral fracture (1.32%) occurred, with a total re-fracture rate of 5.26% (4/76). In control group, the corresponding numbers were 10 new vertebral fractures (13.16%) and 3 non-vertebral fractures (3.95%), with a total re-fracture rate of 17.11% (13/76). The total re-fracture rate in observation group was markedly lower as against control group (5.26% vs 17.11%, $\chi^2 = 9.351$, $p = 0.007$) (Figure 6).

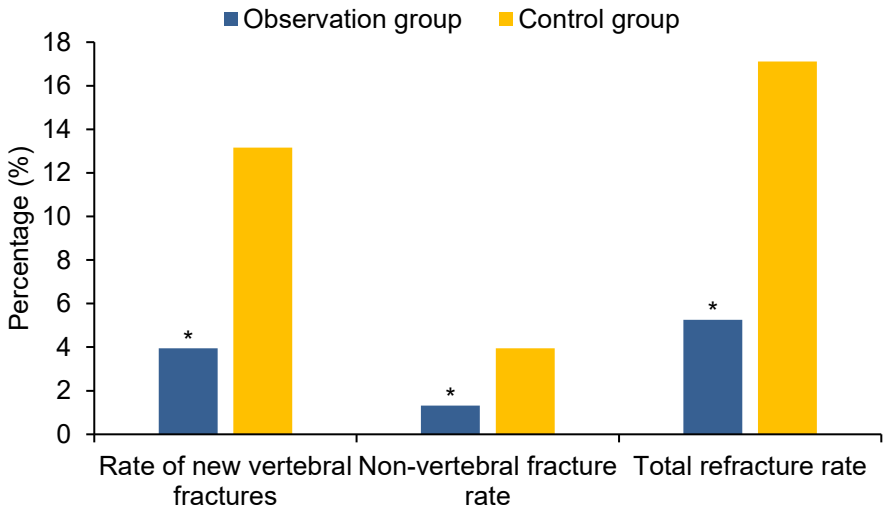

Figure 6.

Contrast of re-fracture rates at 12 months postoperatively. *As against control group, $p < 0.05$

Contrast of adverse reactions

Adverse events mainly included hypocalcemia, gastrointestinal reactions, fever, and headache. In observation group, hypocalcemia was observed in 4 cases (5.26%), gastrointestinal reactions in 6 cases (7.89%), fever in 1 case (1.32%), and headache in 1 case (1.32%), with a total of 12 adverse reactions (15.79%). In control group, hypocalcemia was observed in 6 cases (7.89%), gastrointestinal reactions in 8 cases (10.53%), fever in 1 case (1.32%), and headache in 2 cases (2.63%), with a total of 17 adverse reactions (22.37%). There was no visible distinction in the adverse reactions ($\chi^2 = 1.351$, $p = 0.173$). No severe adverse events occurred in the subjects (Figure 7).

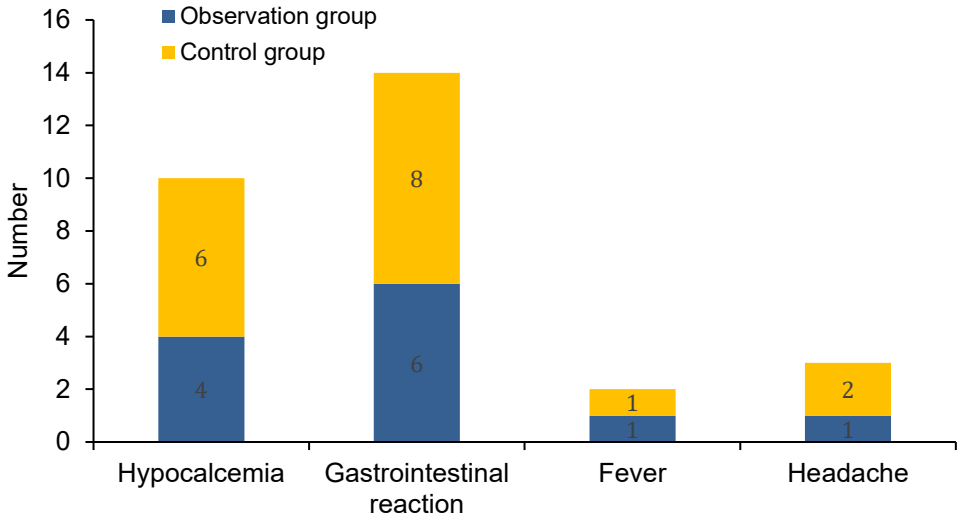

Figure 7.
Contrast of postoperative adverse reactions

This 12-month retrospective follow-up study systematically evaluated the comprehensive efficacy of denosumab combined with calcitriol in elderly OVCF patients after PKP. The results demonstrated that, compared with calcitriol alone, the combined regimen showed significant advantages in improving bone metabolic markers, promoting vertebral morphological restoration, reducing bone cement leakage rates, and lowering the risk of re-fracture, with a favorable safety profile. One of the most pivotal findings of this study is the dual regulatory effect of the combined therapy on bone metabolic balance. Denosumab, as a RANKL inhibitor, potently inhibits osteoclast-mediated bone resorption (reflected by a significant decrease in β-CTX), while calcitriol, by promoting intestinal calcium absorption and directly stimulating osteoblast differentiation, synergistically enhances bone formation activity (reflected by sustained increases in BGP, PINP, and BALP) (22, 23). The results of this study indicate that the combination therapy achieved an ideal bone metabolic state characterized by "high bone formation and low bone resorption." This finding presents a meaningful contrast to the study by Kobayakawa *et al*. (24), which reported that while denosumab monotherapy effectively reduced bone resorption, it might also lead to a decrease in bone formation markers, posing a risk of inducing a "low turnover" state. In the present study, with the addition of calcitriol, bone formation markers were not suppressed but instead showed a sustained increase. This suggests that combining calcitriol in clinical practice may effectively circumvent the potential suppression of osteogenic function by anti-resorptive agents, providing strong evidence for a "dual-target" treatment strategy in osteoporosis.

Another significant and novel finding of this study is the lower bone cement leakage rate observed in the combination therapy group (7.89% *vs*. 14.47%). It was hypothesized that the potential mechanism may be related to the beneficial effect of denosumab on the early stability of the bone-cement interface. Following PKP, the injected bone cement and the surrounding bone tissue form a mechanical composite (25, 26). Osteoclast activity persists in the early postoperative period, and the resulting bone resorption may lead to micromotion and micro-gaps at the cement-bone interface, creating potential pathways for cement leakage (27, 28). By rapidly and potently inhibiting osteoclast activity, denosumab may reduce such interfacial micromotion and microdamage, thereby enhancing the initial stability of the interface and decreasing the risk of cement leakage due to micromovement before and during cement solidification (29, 30). This mechanistic hypothesis is supported by evidence from basic research. As a RANKL inhibitor, denosumab potently suppresses osteoclast activity by blocking the key pathway, elucidated by Boyle *et al*. (31), which is essential for osteoclast differentiation and activation. This inhibition may reduce the early postoperative micromotion and micro-gaps at the bone-cement interface caused by osteoclastic bone resorption, thereby enhancing the initial stability of the interface and consequently reducing the risk of cement leakage. This observation is consistent with the findings of Søballe *et al*. (32) in implant-related research, which also indicated that inhibiting bone resorption improves early stability at the bone-implant interface. The clinical phenomenon observed in this study provides indirect yet insightful clinical evidence for this biological pathway.

In this study, the combination therapy group exhibited a significantly lower refracture rate during the 12-month follow-up (5.26% vs. 17.11%), which aligns with the findings of Black *et al*. (33) that denosumab monotherapy reduces vertebral fracture risk by approximately 50%, yet the risk reduction observed here (approximately 72.6%) was more pronounced. This strongly suggests that the addition of calcitriol not only does not attenuate the efficacy of denosumab but, by promoting bone formation and improving bone quality, produces a synergistic effect. Through dynamic MRI monitoring, this study is the first to confirm a significant positive correlation between the vertebral anterior height restoration rate and bone formation markers (such as BALP), while a negative correlation was observed between Cobb angle deterioration and BMD improvement. This provides imaging evidence that the restoration of bone metabolic balance serves as the biological foundation for long-term vertebral morphological stability.

The results of this study indicate that the combination of denosumab and calcitriol produces a synergistic effect, likely achieved through multi-target regulation of bone metabolic balance. Denosumab inhibits RANKL, curbing excessive bone resorption at its source and creating a stable microenvironment for bone formation (34-36). Calcitriol not only provides ample raw materials for bone mineralization by promoting intestinal absorption of calcium and phosphorus but may also directly stimulate osteoblast activity and indirectly optimize bone remodeling by regulating parathyroid hormone levels (37). This dual regulatory approach of promoting formation and inhibiting absorption together contributed to the ideal state of bone metabolism characterized by high formation and low absorption (38). The resulting clinical benefits are systemic: rapid increases in bone density and improvements in bone quality directly enhance the compressive strength of adjacent vertebrae, thereby reducing the risk of refracture. Meanwhile, the improved quality of local vertebral bone healing is closely associated with long-term vertebral morphological stability and the consolidation of the bone-cement interface (39, 40). This provides an intrinsic and coherent biological explanation for the superiority of the combination therapy over monotherapy.

The deficiencies of this article are as follows: Limited sample size, no subgroup analysis of different doses or timing of medication was included. As a retrospective analysis, patient grouping was not randomized. Although no statistically significant differences were observed in baseline characteristics between the two groups, potential unmeasured confounding factors and selection bias may still exist. Future studies could increase the sample size and combine multi-omics technologies (such as transcriptomics and metabolomics) to explore the precise regulatory targets of combined therapy and further verify its preventive effect on non-vertebral fractures (such as hip fractures).

Conclusions

In this retrospective study, the combination of denosumab and calcitriol can synergistically improve the postoperative bone metabolic imbalance in elderly OVCF patients after PKP, markedly increase bone formation markers and bone density, inhibit bone resorption, and promote vertebral shape recovery, with increased vertebral height recovery rate and stable Cobb angle. The re-fracture rate in the combined therapy group was reduced by 72.6% at 12 months postoperatively compared with the monotherapy group, and the safety was good. This article provided evidence-based support for optimizing the postoperative management of elderly osteoporotic fractures through multidimensional verification by MRI imaging and biochemical indicators, supporting the combination of denosumab and calcitriol as the preferred adjuvant therapy after PKP. These findings suggest that this combination may serve as an effective adjuvant therapy; however, prospective randomized controlled trials are required to confirm these results.

Acknowledgement

Not applicable.

Funding

Not applicable.

Availability of data and materials

The data generated in the present study are included in the figures and/or tables of this article.

Ethics approval and consent to participate

The study was approved by Ethics Committee of Zhejiang Provincial People's Hospital (Zhejiang, China). All participants agreed to sign informed consent forms with the consent of their family members.

AI use disclosure

Not applicable.

Conflict of interest

The authors declare no conflict of interest. / The authors declare that ...

References

1. Imamudeen N, Basheer A, Iqbal AM, Manjila N, Haroon NN, Manjila S. Management of osteoporosis and

spinal fractures: contemporary guidelines and evolving paradigms. Clin Med Res. 2022;20(2):95-106.
2. Li C, Lai XM, Liu N, Lin Y, Hu W. Correlation analysis of the vertebral compression degree and CT HU value in elderly patients with osteoporotic thoracolumbar fractures. J Orthop Surg Res. 2023;18(1):457.
3. Ma Y, Lu Q, Wang X, Wang Y, Yuan F, Chen H. Establishment and validation of a nomogram for predicting new fractures after PKP treatment of osteoporotic vertebral compression fractures in elderly individuals. BMC Musculoskelet Disord. 2023;24(1):728.
4. Chen L, Huang Q. Meta-analysis of efficacy of bisphosphonates in nontraumatic osteonecrosis of femoral head. Farmacia. 2025;73(5):1081-1088.
5. Curtis JR, Arora T, Liu Y, Lin TC, Spangler L, Brunetti VC, et al. Comparative effectiveness of denosumab vs alendronate among postmenopausal women with osteoporosis. J Bone Miner Res. 2024;39(7):826-834.
6. Jeka S, Dokoupilová E, Kivitz A, Żuchowski P, Vogg B, Krivtsova N, et al. Equivalence trial of proposed denosumab biosimilar GP2411 and reference denosumab in postmenopausal osteoporosis: the ROSALIA study. J Bone Miner Res. 2024;39(3):202-210.
7. Widyadharma IPE, Tertia C, Vania A, Tiffani P, Wiratnaya IGE. The effect of denosumab vs. zoledronic acid in preventing skeletal-related events, including pain-related bone metastasis: a systematic review. Postep Psychiatr Neurol. 2024;33(3):172-177.
8. Tan X, Zhang Y, Wei D, Yang Y, Xiang F. Denosumab for giant cell tumors of bone from 2010 to 2022: a bibliometric analysis. Clin Exp Med. 2023;23(7):3053-3075.
9. Zhu K, Zhang J, Zhang C, et al. Therapeutic efficacy of zoledronic acid combined with calcitriol in elderly patients receiving total hip arthroplasty or hemiarthroplasty for osteoporotic femoral neck fracture. Osteoporos Int. 2021;32(3):559-564.
10. El Nekidy WS, Ghazal I, Mallat J, Abidi E, Malik A, Madhyastha R, et al. Efficacy of Alfacalcidol Versus Calcitriol in Managing Secondary Hyperparathyroidism in Patients With Chronic Kidney Disease. Hosp Pharm. 2025;60(4):379-383.
11. Seib CD, Meng T, Cisco RM, Lin DT, McAninch EA, Chen J, et al. Risk of Permanent Hypoparathyroidism Requiring Calcitriol Therapy in a Population-Based Cohort of Adults Older Than 65 Undergoing Total Thyroidectomy for Graves' Disease. Thyroid. 2023;33(2):223-229.
12. Zhang Y, Tian Y, Chen X. Therapeutic efficacy of zoledronic acid combined with calcium and calcitriol in the treatment of senile osteoporosis in elderly patients. Inflammopharmacology. 2025;33(4):1899-1905.
13. Herrera-Martínez Y, Contreras González MJ, Pedraza-Arévalo S, Guerrero Martínez MDC, Rodrigo Martínez Á, González Menchen A, et al. Calcitriol-Mediated Hypercalcemia, Somatostatin Receptors Expression and 25-Hydroxyvitamin D3-1α- Hydroxylase in GIST Tumors. Front Endocrinol (Lausanne). 2022;12:812385.
14. Zhang ZL, Liao EY, Xia WB, et al. Alendronate sodium/vitamin D3 combination tablet versus calcitriol for osteoporosis in Chinese postmenopausal women: a 6-month, randomized, open-label, active-comparator-controlled study with a 6-month extension. Osteoporos Int. 2015;26(9):2365-2374.
15. Bao C, Luo J, Meng Y, Gao Z. Effects of paeoniflorin extract-mediated miRNA-140 targeting of wnt/β-catenin signalling pathway on proliferation and apoptosis of chondrocytes in osteoarthritis. Farmacia. 2025;73(6):1605-1615.
16. Lombardi AF, Aihara AY, Fernandes ADRC, Cardoso FN. Imaging of Paget's disease of bone. Radiol Clin North Am. 2022;60(4):561-573.
17. Yamamoto N, Shiroshita A, Kimura R, Kamo T, Ogihara H, Tsuge T. Diagnostic accuracy of chest X-ray and CT using artificial intelligence for osteoporosis: systematic review and meta-analysis. J Bone Miner Metab. 2024;42(5):483-491.
18. Salzmann SN, Okano I, Jones C, et al. Preoperative MRI-based vertebral bone quality (VBQ) score assessment in patients undergoing lumbar spinal fusion. Spine J. 2022;22(8):1301-1308.
19. Kircher K, Chaudry O, Nagel AM, et al. Effects of high-intensity training on fatty infiltration in paraspinal muscles in elderly males with osteosarcopenia: the randomized controlled FrOST study. BMC Geriatr. 2024;24(1):141.
20. Qin J, Zhong W, Quan Z. The surgical management trends of osteoporotic vertebral compression fractures: 5-year experience in one institution. Sci Rep. 2022;12(1):18040.
21. Heilbronner AK, Koff MF, Breighner R, et al. Opportunistic evaluation of trabecular bone texture by MRI reflects bone mineral density and microarchitecture. J Clin Endocrinol Metab. 2023;108(8):e557-e566.
22. Kendler DL, Bone HG, Massari F, et al. Bone mineral density gains with a second 12-month course of romosozumab therapy following placebo or denosumab. Osteoporos Int. 2019;30(12):2437-2448.
23. Stathi D, Fountoulakis N, Panagiotou A, et al. Impact of treatment with active vitamin D calcitriol on bone turnover markers in people with type 2 diabetes and stage 3 chronic kidney disease. Bone. 2023;166:116581.
24. Kobayakawa T, Miyazaki A, Saito M, Suzuki T, Takahashi J, Nakamura Y. Denosumab versus romosozumab for postmenopausal osteoporosis treatment. Sci Rep. 2021;11(1):11801.
25. Belkoff SM, Mathis JM, Jasper LE, Deramond H. The biomechanics of vertebroplasty: the effect of cement volume on mechanical behavior. Spine (Phila Pa 1976). 2001;26(14):1537-1541.
26. Tan L, Wen B, Guo Z, Chen Z. The effect of bone cement distribution on the outcome of percutaneous vertebroplasty: a case cohort study. BMC Musculoskelet Disord. 2020;21(1):541.
27. Niu Q, Gao J, Wang L, Liu J, Zhang L. Regulation of differentiation and generation of osteoclasts in rheumatoid arthritis. Front Immunol. 2022;13:1034050.
28. Zainal Ariffin SH, Lim KW, Megat Abdul Wahab R, et al. Gene expression profiles for in vitro human stem cell differentiation into osteoblasts and osteoclasts: a systematic review. PeerJ. 2022;10:e14174.
29. Vaculik J, Wenchich L, Bobelyak M, Pavelka K, Stepan JJ. Decrease in serum calcitriol (but not free 25-hydroxyvitamin D) concentration in hip fracture healing. J Endocrinol Invest. 2021;44(9):1847-1855.
30. Wan J, Xie J, Hu C, Liu J, Zhu C. Effect of calcium plus vitamin-D combined with calcitriol in the treatment of

patients with type-2 diabetes and osteoporosis: a retrospective observational analysis. Pak J Med Sci. 2024;40(3Part-II):444-448.
31. Boyle WJ, Simonet WS, Lacey DL. Osteoclast differentiation and activation. Nature. 2003;423(6937):337-342.
32. Søballe K. Hydroxyapatite ceramic coating for bone implant fixation: mechanical and histological studies in dogs. Acta Orthop Scand Suppl. 1993;255:1-58.
33. Black DM, Delmas PD, Eastell R, et al. Once-yearly zoledronic acid for treatment of postmenopausal osteoporosis. N Engl J Med. 2007;356(18):1809-1822.
34. Han K, Wang X. Clinical efficacy and outcomes of calcitriol combined with bisphosphonates in the treatment of postmenopausal osteoporosis: a quasi-experimental study. Medicine (Baltimore). 2024;103(45):e40171.
35. Brănescu C, Serban D, Dascălu AM, Oprescu SM, Savlovschi C. Interleukin 6 and lipopolysaccharide binding protein - markers of inflammation in acute appendicitis. Chirurgia (Bucur). 2013;108(2):206-14.
36. Zhang Y, Tian Y, Chen X. Therapeutic efficacy of zoledronic acid combined with calcium and calcitriol in the treatment of senile osteoporosis in elderly patients. Inflammopharmacology. 2025;33(4):1899-1905.
37. Wu W, Zheng W, Pan W, Chen F, Jiang L. Reducing re-fractures post percutaneous kyphoplasty: the impact of zoledronic acid with calcium and vitamin D3 in osteoporotic patients. Altern Ther Health Med. 2024;30(12):340-345.
38. Chen CL, Chen NC, Liang HL, Hsu CY, Chou KJ, Fang HC, Lee PT. Effects of Denosumab and Calcitriol on Severe Secondary Hyperparathyroidism in Dialysis Patients With Low Bone Mass. J Clin Endocrinol Metab. 2015;100(7):2784-92.
39. Graul I, Marintschev I, Hackenbroch C, Palm HG, Friemert B, Lang P. Modified therapy concepts for fragility fractures of the pelvis after additional MRI. PLoS One. 2020;15(10):e0238773.
40. Shi C, Zhang M, Cheng AY, Huang ZF. Percutaneous kyphoplasty combined with zoledronic acid infusion in the treatment of osteoporotic thoracolumbar fractures in the elderly. Clin Interv Aging. 2018;13:853-861.